

Electronic Supplementary Material (ESI) for

Tuning circularly polarized luminescence of polymer-stabilized cholesteric liquid crystal films using chiral dopants

Xiaohui Lu, Ziqing Zhou, Baining Ni, Hongkun Li, Yi Li, Baozong Li, Wei Liu*, Yong Wang* and Yonggang Yang*

State and Local Joint Engineering Laboratory for Novel Functional Polymeric Materials, Jiangsu Key Laboratory of Advanced Functional Polymer Design and Application, Jiangsu Engineering Laboratory of Novel Functional Polymeric Materials, Department of Polymer Science and Engineering, College of Chemistry, Chemical Engineering and Materials Science, Key Laboratory of Polymeric Materials Design and Synthesis for Biomedical Function, Soochow University, Suzhou 215123, China. E-mail: weiliu@suda.edu.cn, yowang@suda.edu.cn, ygyang@suda.edu.cn.

Table of contents

Experimental Section	S2-S5
References	S5
Table S1 Crystal measurement and refinement data for TPE-BF₂acac-MeIP	S6
Table S2 Geometrical parameters for C–H···F contacts in the crystal of TPE-BF₂acac-MeIP	S7
Table S3 Optical data of TPE-acac-MeIP and TPE-BF₂acac-MeIP in different solvents	S7
Table S4 Calculated optical transitions of TPE-acac-MeIP and TPE-BF₂acac-MeIP	S7
Table S5 Optical data of TPE-acac-MeIP and TPE-BF₂acac-MeIP in solid-state	S8
Table S6 Mass percentages of compounds in the prepolymerized mixtures	S8
Table S7 Bragg reflection properties of <i>R/S</i> CLC films	S8
Table S8 Quantum yields (Φ_F) of <i>R/S</i> CLC films	S8
Table S9 Compounds mass percentages in prepolymerized mixtures with different wt% of dye	S9
Fig. S1 Crystal packing of TPE-BF₂acac-MeIP	S9
Fig. S2 Optical spectra of TPE-acac-MeIP and TPE-BF₂acac-MeIP in different solvents	S10
Fig. S3 Energy level diagram of frontier molecular orbitals and orbital distributions	S10
Fig. S4 Emission spectra of TPE-acac-MeIP in solid states	S11
Fig. S5 PXRD of TPE-BF₂acac-MeIP	S11
Fig. S6 Emission spectra of <i>R</i> -CLC films and <i>S</i> -CLC films	S12
Fig. S7 Photographs and DRUV-vis spectra of <i>S</i> -CLC films with different structural colours	S12
Fig. S8 POM images	S13
Fig. S9 FESEM images the <i>R</i> -CLC films with 2.00, 1.75, 1.50, and 1.30 wt% <i>R</i> 5011	S13
Fig. S10 CD of TPE-BF₂acac-MeIP in (<i>R</i>)/(<i>S</i>)-phenylethanol and DRCD of <i>R/S</i> -Red CLC films	S13
Fig. S11 DRUV-vis and transmittance spectra of <i>R</i> -Dark Green CLC films	S14
Fig. S12-19 ESI-MS, ¹ H NMR, ¹³ C NMR, and FT-IR spectra	S15-18

Experimental Section

Materials and instruments

Tetrakis(triphenylphosphine)palladium, 2-aminopyridine, NaH, ⁿBu₄NBr, and BF₃•Et₂O were purchased from Energy Chemical Co., Ltd. Acetylacetone and K₂CO₃ were purchased from Sinopharm Group Co. Ltd. N-bromosuccinimide (NBS) was purchased from Shanghai Aladdin Biochemical Technology Co., Ltd. 2-Bromo-1,1,2-triphenylethylene was purchased from Shanghai Macklin Biochemical Co., Ltd. **C6M**, **RM105**, **R-5011** and **S-5011** were purchased from Sanjiang advanced materials R&D Co., Ltd. **BDK** was purchased from Adamas Chemical Co., Ltd. Methyl 4-boronobenzoate was purchased from Accela ChemBio Co., Ltd. Solvents were distilled with standard methods.

FT-IR spectra of solid samples were performed in the range of 400–4000 cm⁻¹ on a Bruker VRETEX 70 spectrometer at 4.0 cm⁻¹ resolution by an averaging over 16 scans. Mass spectra were recorded on Bruker micro TOF-Q III and Agilent Technologies 6220 Accurate-Mass TOF LC/MS. ¹H NMR and ¹³C NMR were recorded with Agilent-400 and Bruker-400 spectrometers in CDCl₃ at ambient temperature. Chemical shifts (δ , ppm) were reported with respect to residual solvent peaks as internal standard (¹H: chloroform, δ = 7.26 ppm; ¹³C: chloroform, δ = 77.2 ppm). The UV–vis absorption spectra and DRUV-vis reflectance spectra were carried out on UV-VIS-NIR spectrophotometer (UV3600). Emission measurements were recorded with FLS920 fluorescence spectrometer at the solution and the solid-state. The absolute fluorescence quantum yields for samples and films were measured on FLS 980 (Edinburgh Instrument, UK). The POM images of the target compounds were taken using a Leica Microsystems CMS GmbH fitted with a Linkam LTS420 hot stage. Circular dichroism (CD) spectra for solutions were obtained on a JASCO J-1500 spectrometer (Tokyo, Japan), with a bandwidth of 2.0 nm, a 0.5 nm-interval, an average scanning speed of 200 nm/min, and a 2-mm cell at 25°C. Diffuse reflectance circular dichroism (DRCD) spectra were measured by using a JASCO 815 spectrometer (JASCO, Japan), and anhydrous barium sulfate dried at a high temperature was used as blank. CPL spectra were measured on JASCO CPL-300 (Tokyo, Japan), with an excitation wavelength of 400 nm, a scan speed of 200 nm/min, number of scans of 1, and slit width of 3000 μ m at 25°C. To eliminate the effect of linearly polarized luminescence, CPL spectra of the films were measured by using a plate holder allowing the samples to be rotated through 360° at 22.5° increments. 1-(2-methylimidazo[1,2-*a*]pyridin-3-yl)ethan-1-one (**MeIP-COMe**) and methyl 4-(1,2,2-triphenylvinyl)benzoate (**TPE-COOMe**) were prepared according to the previously reported method.^{S1, S2}

Computation details

All calculations were carried out with Gaussian 09 programs.^{S3} The optimizations were started from the geometries of **TPE-acac-MeIP** and **TPE-BF₂acac-MeIP** obtained by X-ray diffraction. Density functional theory (DFT) and time-dependent DFT (TDDFT) were carried out at the B3LYP functional level by using 6-31G(d) for all atoms.^{S4-6}

X-ray crystallography

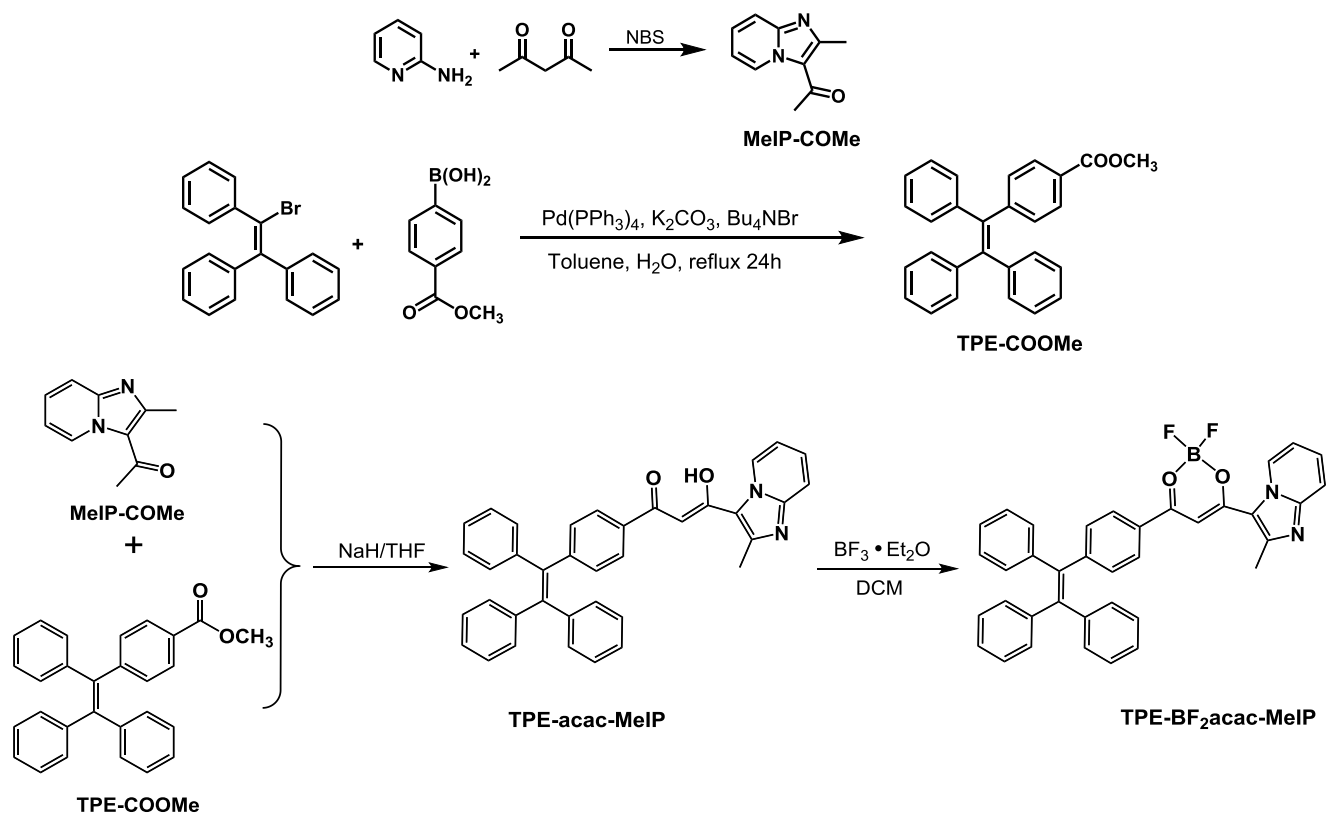
Orange-red single crystals of **TPE-BF₂acac-MeIP** grown from concentrated CH₃CN/EtOAc (v/v, 1/1) solutions at room temperature were selected and mounted on a glass fiber. Crystal determination was performed with a Bruker SMART APEX II CCD diffractometer equipped with graphite-monochromated Mo K α radiation ($\lambda = 0.71073 \text{ \AA}$). The structures were solved by direct methods and refined by full-matrix least squares methods on F^2 using SHELX^{S7} under OLEX2.^{S8} The hydrogen atoms were assigned with common isotropic displacement factors, and included in the final refinement by use of geometrical restraints. CCDC 210127 contains the supplementary crystallographic data for this paper. These data can be obtained free of charge from the Cambridge Crystallographic Data Centre via www.ccdc.cam.ac.uk/data_request/cif.

Preparation for AIE study

A stock solution of sample **TPE-BF₂acac-MeIP** (1 mM) was prepared in THF, and 20 μL of this stock solution was transferred to a 10 mL volumetric flask. After adding proper amounts of THF, deionized water was then added slowly under sonication to afford 10 μM solutions with different water volume fractions. The emission spectra of the prepared solutions were measured immediately.

Preparation for liquid crystal thin films

Reactive CLC mesogens **C6M** and **RM105**, photoinitiator **BDK**, chiral dopants **R/S5011**, and dye **TPE-BF₂acac-MeIP** were dissolved in dichloromethane according to the weight ratios listed in Table S6. The solvent was then evaporated completely on the surface of a quartz plate at 120°C for 5 min. The thickness of the liquid layer was kept at 11 μm , by using an 11 μm spacer in the middle between two quartz plates. After the temperature of the liquid layer was cooled down to 90°C, a 365 nm-xenon lamp irradiation was carried out (10 seconds) for photopolymerization. Then free-standing *R/S*-CLC films were obtained and peeled off from the quartz plates with a blade.



Scheme S1. Synthetic routes of compounds **TPE-acac-MeIP** and **TPE-BF₂acac-MeIP**.

Synthesis of compound **TPE-acac-MeIP**.

Under a N₂ atmosphere, to a THF solution (40 mL) of 1-(2-methylimidazo[1,2-*a*]pyridin-3-yl)ethan-1-one (**MeIP-COMe**, 0.45 g, 2.60 mmol) in a three-necked flask, NaH (0.60 g, 10.2 mmol) was added. The mixture was refluxed with stirring for 2 h, and the mixture changed from colorless to dark-red. Methyl 4-(1,2,2-triphenylvinyl)benzoate (**TPE-COOMe**, 1.30 g, 3.30 mmol) was added, and the reaction was continued for 24 h. After the reaction was complete which was confirmed by TLC, the mixture was cooled to room temperature, and poured into ice water and acidified with HCl (2 M) to pH ≈ 5-6. After extraction with dichloromethane (3 × 40 mL), the organic phase was dried over anhydrous Na₂SO₄. The solvent was evaporated, and the residue was purified by column chromatography (silica gel, EtOAc/petroleum ether, v/v = 1:1) to give a yellow powder of **TPE-acac-MeIP**. Yield: 45% (0.60 g). m. p. 164.2–165.2°C. FT-IR (ATR, cm⁻¹): 1603, 1443, 787, 659. ¹H NMR (400 MHz, CDCl₃): δ 16.59 (s, 1H), 9.66 (d, *J* = 7.2 Hz, 1H), 7.66 (s, 3H), 7.41 (s, 1H), 7.12 (s, 10H), 7.04 (s, 8H), 6.58 (s, 1H), 2.82 (s, 3H). ¹³C NMR (101 MHz, CDCl₃): δ 182.6, 177.1, 150.9, 148.0, 147.0, 143.3, 143.2, 143.2, 142.4, 132.1, 131.7, 131.3, 129.3, 128.5, 127.9, 127.8, 127.7, 126.9, 126.7, 125.9, 120.0, 116.7, 114.1, 95.1, 18.3. ESI-MS (*m/z*): 533.2218, Calcd. exact mass for C₃₇H₂₉N₂O₂⁺ ([M+H]⁺): 533.2224. Calcd. for C₃₇H₂₈N₂O₂: C, 83.43, H, 5.30, N, 5.26. Found: C, 82.46, H, 5.46, N, 5.26.

Synthesis of compound **TPE-BF₂acac-MeIP**.

Under N₂, BF₃•Et₂O (0.35 mL, 2.75 mmol) was added dropwise to a solution of **TPE-acac-MeIP** (0.30 g, 0.55 mmol) in anhydrous CH₂Cl₂ (30 mL). The mixture was stirred at 50°C for 5 h. After quenching the reaction with water, the mixture was extracted with dichloromethane, and dried over anhydrous Na₂SO₄. The solvent was evaporated, and the crude product was recrystallized in EtOAc to afford an orange powder. Yield: 91% (0.33 g). m. p. > 260°C FT-IR (ATR, cm⁻¹): 1556, 1273, 701. ¹H NMR (400 MHz, CDCl₃): δ 9.52 (d, *J* = 7.0 Hz, 1H), 7.81 (d, *J* = 8.3 Hz, 2H), 7.73 (d, *J* = 8.7 Hz, 1H), 7.61 (t, *J* = 7.9 Hz, 1H), 7.20 (s, 1H), 7.18–7.11 (m, 12H), 7.07–7.01 (m, 6H), 6.84 (s, 1H), 2.87 (s, 3H). ¹³C NMR (100 MHz, CDCl₃): δ 182.6, 177.1, 150.9, 148.0, 147.0, 143.3, 143.2, 142.4, 132.1, 131.7, 131.3, 129.3, 128.5, 127.9, 127.8, 127.7, 126.9, 126.7, 125.9, 120.0, 116.7, 114.1, 95.1, 18.3. ESI-MS (*m/z*): 581.2143, Calcd. exact mass for C₃₇H₂₈BF₂N₂O₂⁺ ([M+H]⁺): 581.2206. Calcd. for C₃₇H₂₈BF₂N₂O₂: C, 76.56, H, 4.69, N, 4.83. Found: C, 76.01, H, 4.80, N, 4.80.

References

- S1. S. B. Bhagat and V. N. Telvekar, *Tetrahedron Lett.*, 2017, **58**, 3662–3666.
- S2. H. Gao, D. Xu, X. Liu, A. Han, L. Zhou, C. Zhang, Z. Li and J. Dang, *Dyes Pigm.*, 2017, **139**, 157–165.
- S3. M. J. Frisch, G. W. Trucks, H. B. Schlegel, G. E. Scuseria, M. A. Robb, J. R. Cheeseman, G. Scalmani, V. Barone, B. Mennucci, G. A. Petersson, H. Nakatsuji, M. Caricato, X. Li, H. P. Hratchian, A. F. Izmaylov, J. Bloino, G. Zheng, J. L. Sonnenberg, M. Hada, M. Ehara, K. Toyota, R. Fukuda, J. Hasegawa, M. Ishida, T. Nakajima, Y. Honda, O. Kitao, H. Nakai, T. Vreven, J. A. J. Montgomery, J. E. Peralta, F. Ogliaro, M. Bearpark, J. J. Heyd, E. Brothers, K. N. Kudin, V. N. Staroverov, R. Kobayashi, J. Normand, K. Raghavachari, A. Rendell, J. C. Burant, S. S. Iyengar, J. Tomasi, M. Cossi, N. Rega, J. M. Millam, M. Klene, J. E. Knox, J. B. Cross, V. Bakken, C. Adamo, J. Jaramillo, R. Gomperts, R. E. Stratmann, O. Yazyev, A. J. Austin, R. Cammi, C. Pomelli, J. W. Ochterski, R. L. Martin, K. Morokuma, V. G. Zakrzewski, G. A. Voth, P. Salvador, J. J. Dannenberg, S. Dapprich, A. D. Daniels, O. Farkas, J. B. Foresman, J. V. Ortiz, J. Cioslowski and D. J. Fox, *Gaussian 09, revision D.01 Gaussian, Inc.: Wallingford, CT*, 2013.
- S4. C. Lee, W. Yang and R. G. Parr, *Phys. Rev. B*, 1988, **37**, 785–789.
- S5. B. Miehlich, A. Savin, H. Stoll and H. Preuss, *Chem. Phys. Lett.*, 1989, **157**, 200–206.
- S6. A. D. Becke, *J. Chem. Phys.*, 1993, **132**, 5648–5652.
- S7. G. M. Sheldrick, *Acta Crystallogr A*, 2008, **64**, 112–122.
- S8. O. V. Dolomanov, L. J. Bourhis, R. J. Gildea, J. A. K. Howard and H. Puschmann, *J. Appl. Crystallogr.*, 2009, **42**, 339–341.

Table S1 Crystal measurement and refinement data for **TPE-BF₂acac-MeIP**.

CCDC Number	2101277
Empirical formula	C ₃₇ H ₂₇ BF ₂ N ₂ O ₂
Formula weight	580.46
Temperature/K	296.15
Crystal system	monoclinic
Space group	C2/c
<i>a</i> /Å	35.867(3)
<i>b</i> /Å	8.0882(5)
<i>c</i> /Å	19.9608(15)
α /°	90
β /°	100.844(2)
γ /°	90
Volume/Å ³	5687.2(7)
Z	8
ρ_{calc} g/cm ³	1.3557
μ /mm ⁻¹	0.092
<i>F</i> (000)	2417.2
Crystal size/mm ³	0.6 × 0.4 × 0.2
Radiation	Mo K α (λ = 0.71073)
2 θ range for data collection/°	4.36 to 50
Index ranges	-38 ≤ <i>h</i> ≤ 46, -10 ≤ <i>k</i> ≤ 10, -25 ≤ <i>l</i> ≤ 22
Reflections collected	32288
Independent reflections	5015 [<i>R</i> _{int} = 0.0915, <i>R</i> _{sigma} = 0.1019]
Data/restraints/parameters	5015/1/398
Goodness-of-fit on <i>F</i> ²	1.071
Final <i>R</i> indexes [<i>I</i> ≥ 2 σ (<i>I</i>)]	<i>R</i> ₁ = 0.0536, <i>wR</i> ₂ = 0.1210
Final <i>R</i> indexes [all data]	<i>R</i> ₁ = 0.1064, <i>wR</i> ₂ = 0.1431
Largest diff. peak/hole / e Å ⁻³	0.43/-0.54

Table S2 Geometrical parameters for C–H...F contacts in the crystal of **TPE-BF₂acac-MeIP**.

Contacts	H...F (Å)	C...F (Å)	C–H...F (deg)	Symmetry operation
C3–H3...F1	2.769(5)	3.336(5)	120.3	x, -1+y, z
C5–H5...F2	2.849(0)	3.459(9)	124.3	1-x, y, 1.5-z
C6–H6...F2	2.854(1)	3.584(9)	133.6	1-x, 1-y, 2-z
C13–H13...F2	2.515(1)	3.173(7)	128.0	1-x, 1-y, 2-z

Table S3 Optical data of **TPE-acac-MeIP** and **TPE-BF₂acac-MeIP** measured in different solvents (ca. 20 μM).

Compound	Solvent	$\lambda_{abs}^{max} / \text{nm}^a$	$\lg \epsilon^b$	$\lambda_{em}^{max}(\lambda_{ex}) / \text{nm}$	Stokes shift/cm ⁻¹
TPE-acac-MeIP	DMSO	403	4.6	495 (400)	4610
	CH ₃ CN	396	4.6	487 (400)	4720
	THF	400	4.7	477 (400)	4040
	CH ₂ Cl ₂	399	4.6	484 (400)	4400
	Tol	400	4.7	473 (400)	3860
TPE-BF₂acac-MeIP	DMSO	461	4.5	622 (455)	5610
	CH ₃ CN	453	4.4	619 (455)	5920
	THF	456	4.6	555 (455)	3910
	CH ₂ Cl ₂	457	4.5	595 (455)	5080
	Tol	459	4.6	519 (455)	2520

^a All of the values correspond to the strongest absorption peaks. ^b Molar absorption coefficients are in the maximum of the highest peak.

Table S4 Main calculated optical transitions for **TPE-acac-MeIP** and **TPE-BF₂acac-MeIP** at the level of B3LYP/6-31G(d).

Compound	Orbital excitation	Composition	f^a	λ^b / nm (calcd.)	λ^c / nm (exptl. in CH ₂ Cl ₂)
TPE-acac-MeIP	HOMO → LUMO	0.70266	0.7416	408	400
	HOMO → LUMO	0.70404	0.5094	462	457
TPE-BF₂acac-MeIP	HOMO-1 → LUMO	0.68987	0.7192	368	340 (sh)
	HOMO → LUMO+1	0.65508	0.2321	331	

^a Oscillator strength; ^b Calculated peaks of UV–vis spectra; ^c Experimental data of UV–vis spectra in THF solution.

Table S5 Optical data for **TPE-acac-MeIP** and **TPE-BF₂acac-MeIP** measured in solid-state.

Compound	TPE-acac-MeIP	TPE-BF ₂ acac-MeIP
$\lambda_{\text{em}}^{\text{max}} / \text{nm}$	503	558
$\Phi_{\text{F}}^{\text{a}} \%$	6.8	54.5
$\tau^{\text{b}} / \text{ns}$	1.9	14.2
$k_{\text{r}}^{\text{c}} (10^9 \text{ s}^{-1})$	0.036	0.038
$k_{\text{nr}}^{\text{d}} (10^9 \text{ s}^{-1})$	0.49	0.032

^a Fluorescence quantum yields (Φ) are measured by the absolute method. ^b Emission lifetime collected at their respective emission maxima. ^c Radiative decay constants $k_{\text{r}} = \Phi_{\text{F}}/\tau$. ^d Non-radiative decay constants $k_{\text{nr}} = (1-\Phi_{\text{F}})/\tau$.

Table S6 The mass percentages of compounds in the pre-polymerized mixtures.

Compound	Color			
	Blue	Dark Green	Green	Red
C6M	75.00	75.25	75.50	75.70
RM105	20.00	20.00	20.00	20.00
TPE-BF₂acac-MeIP	2.00	2.00	2.00	2.00
BDK	1.00	1.00	1.00	1.00
R/S5011	2.00	1.75	1.50	1.30

Table S7 Bragg reflection properties of R/S CLC films.

Films	λ (nm) ^a	n ^b	c ^c	p (nm) ^d	β_{m} (μm^{-1}) ^e
R/S-Red	659/655	1.48	1.30	445/443	173/174
R/S-Green	555/556	1.48	1.50	375/376	178/177
R/S-Dark Green	520/522	1.48	1.75	351/353	163/162
R/S-Blue	454/452	1.48	2.00	307/305	163/164

^a λ_{max} values of the CLC films. ^b refractive indices of the CLC films. ^c The mass ratio of the chiral dopants in the CLC films. ^d Helical pitches of the CLC films. ^e The calculated HTP values of R/S5011 ($\beta_{\text{m}} = \text{p}^{-1}\text{c}^{-1}$).

Table S8 Quantum yields (Φ_{F}) of R/S CLC films.

$\Phi_{\text{F}}\%$	Color			
	Blue	Dark Green	Green	Red
R-CLC	63.9	58.7	61.5	50.6
S-CLC	58.2	60.9	64.2	52.8

Table S9 The mass percentages of compounds in the pre-polymerized mixtures for *R*-Dark Green CLC films with different amounts of **TPE-BF₂acac-MeIP**.

Compound	Color		
	Dark Green	Dark Green	Dark Green
C6M	75.25	76.25	76.75
RM105	20.00	20.00	20.00
TPE-BF₂acac-MeIP	2.00	1.00	0.50
BDK	1.00	1.00	1.00
R5011	1.75	1.75	1.75

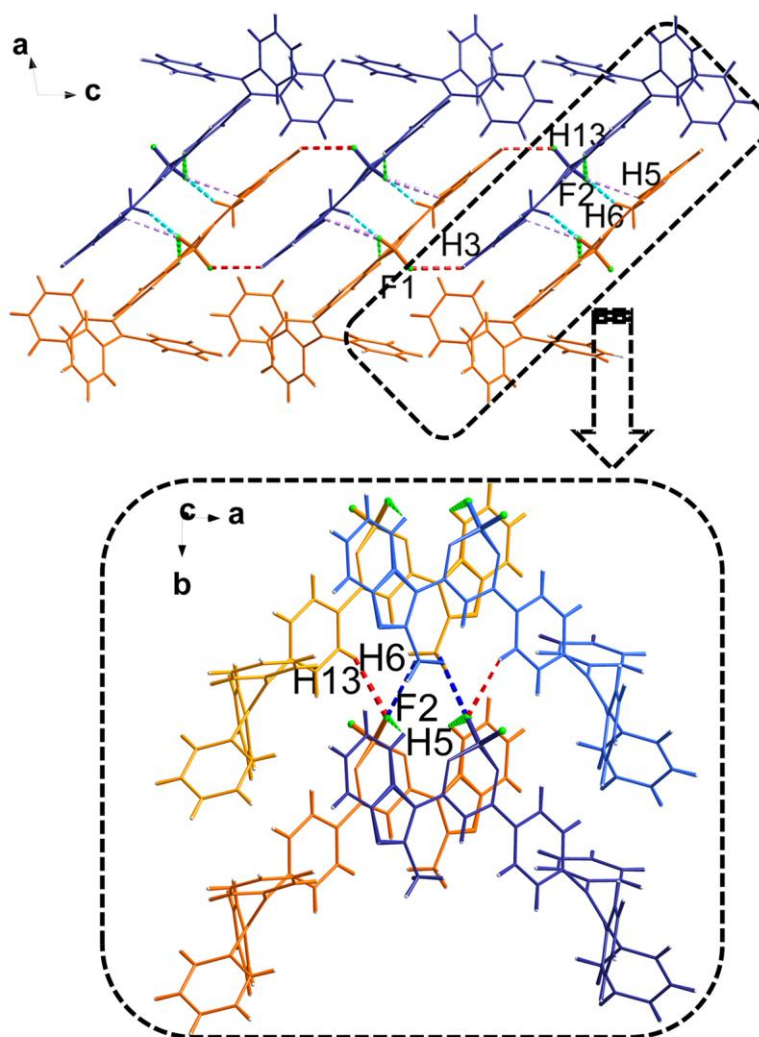


Fig. S1 Crystal packing of **TPE-BF₂acac-MeIP**. Hydrogen contacts are indicated by dashed lines.

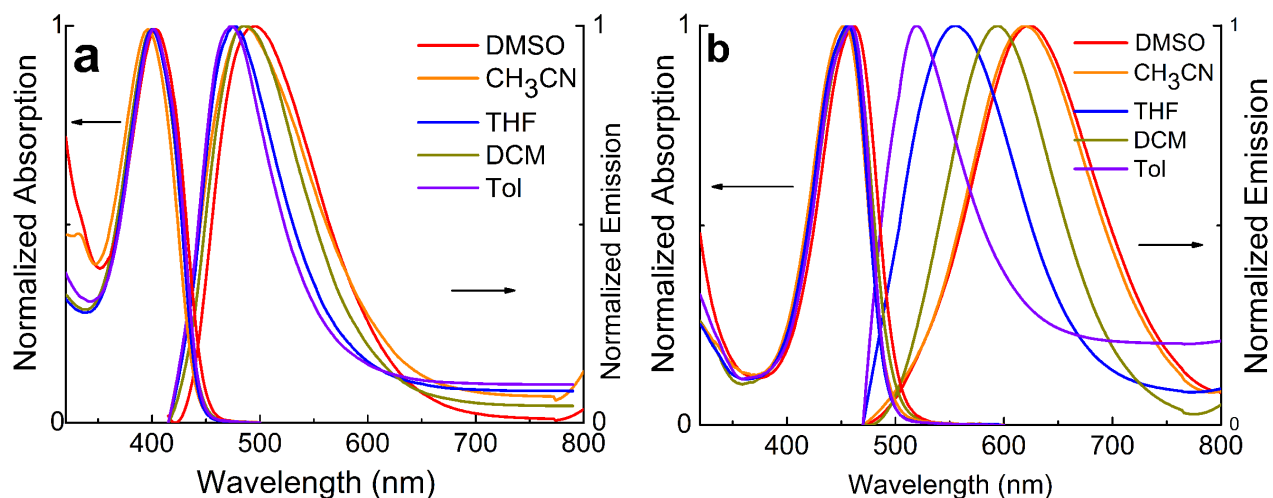


Fig. S2 UV-vis absorption and emission spectra of **TPE-acac-MeIP** and **TPE-BF₂acac-MeIP** in different solvents (20 μ M).

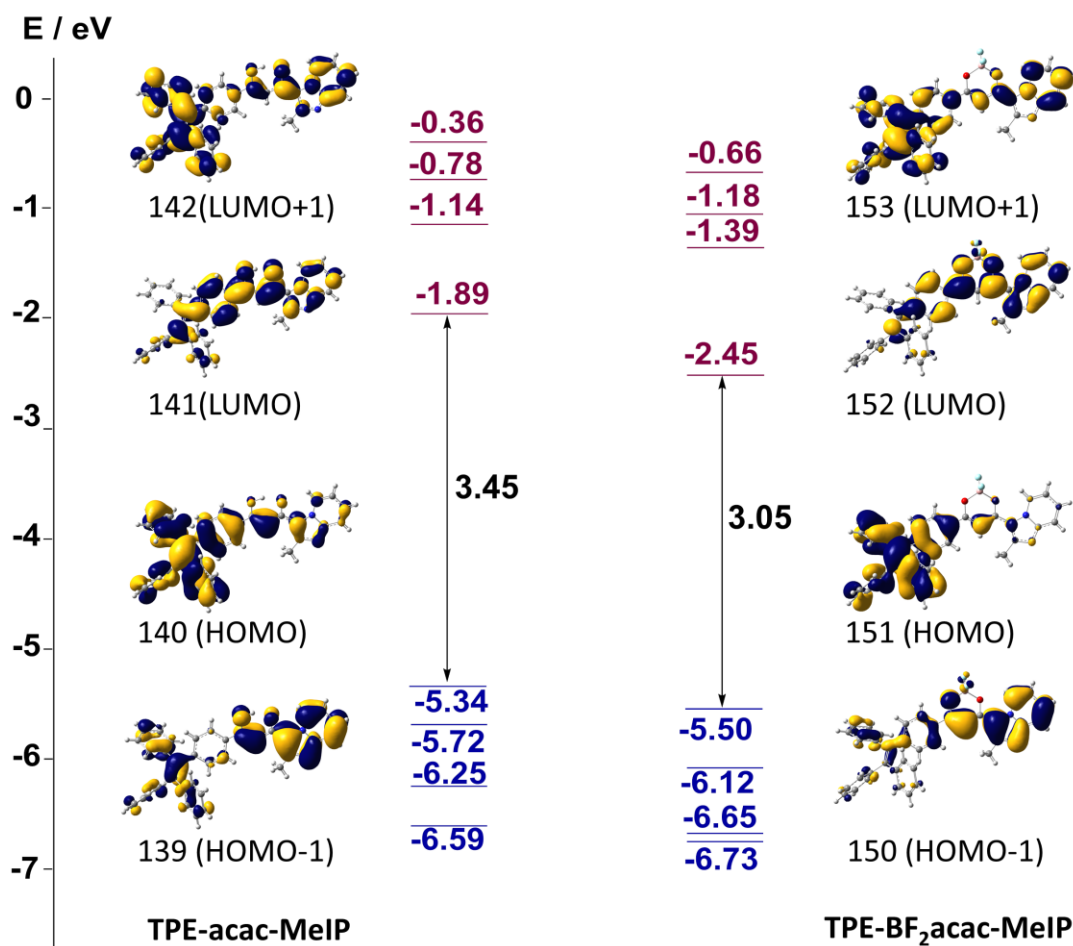


Fig. S3 Energy level diagram of some frontier molecular orbitals, and orbital distributions for **TPE-acac-MeIP** and **TPE-BF₂acac-MeIP**.

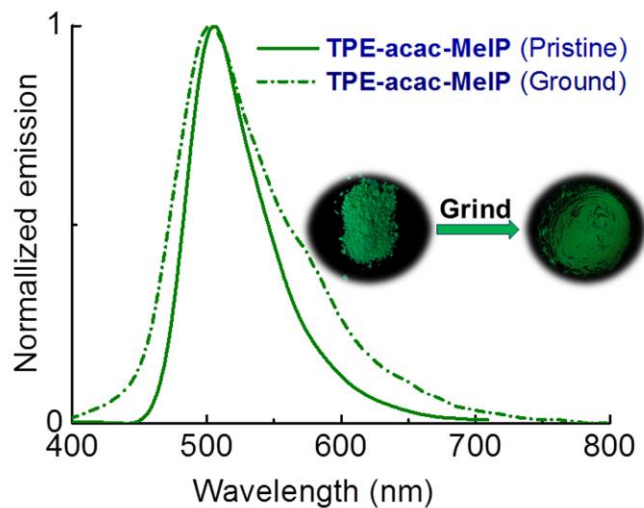


Fig. S4 Emission spectra of **TPE-acac-MeIP** in different solid states ($\lambda_{\text{ex}} = 360 \text{ nm}$), and photos taken with UV-lamp irradiated at 365 nm.

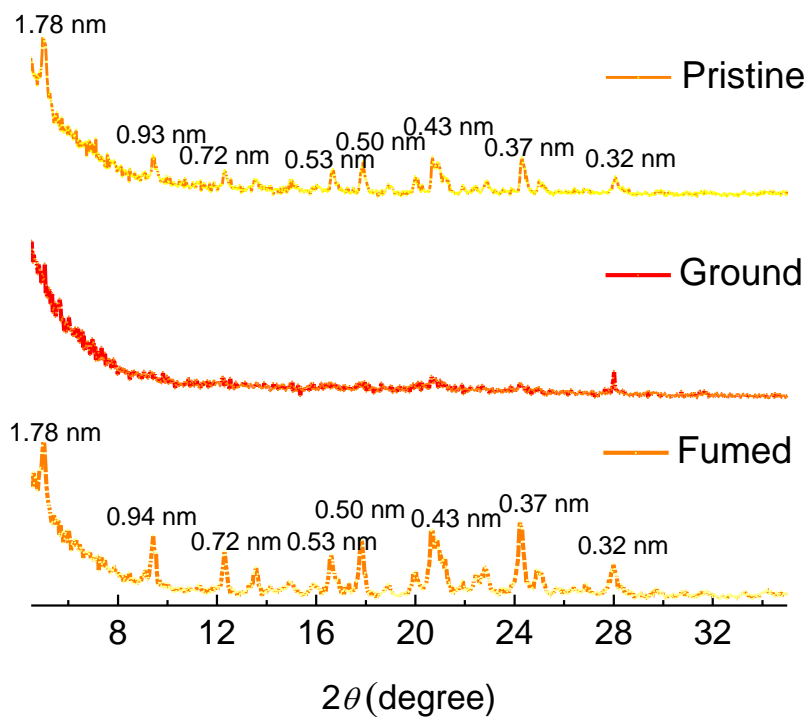


Fig. S5 PXRD results of **TPE-BF₂acac-MeIP**.

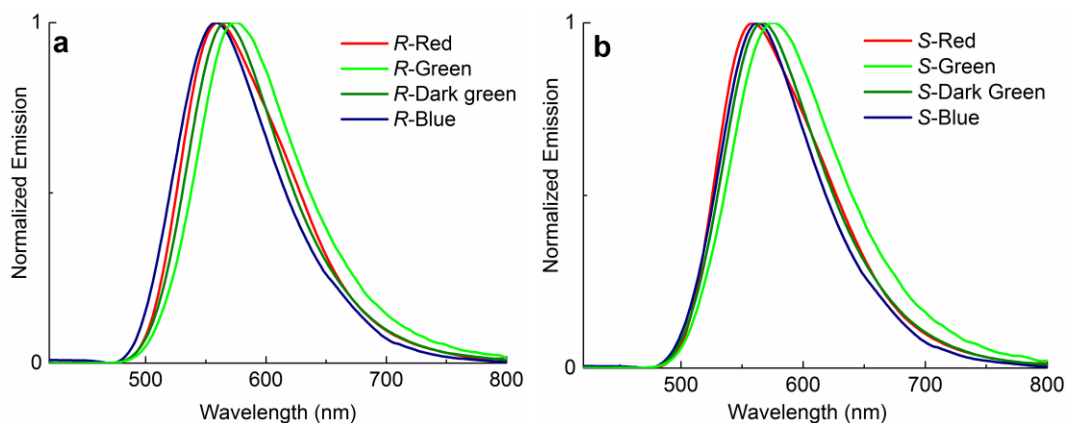


Fig. S6 Emission spectra of (a) *R*-CLC films and (b) *S*-CLC films ($\lambda_{\text{ex}} = 400$ nm).

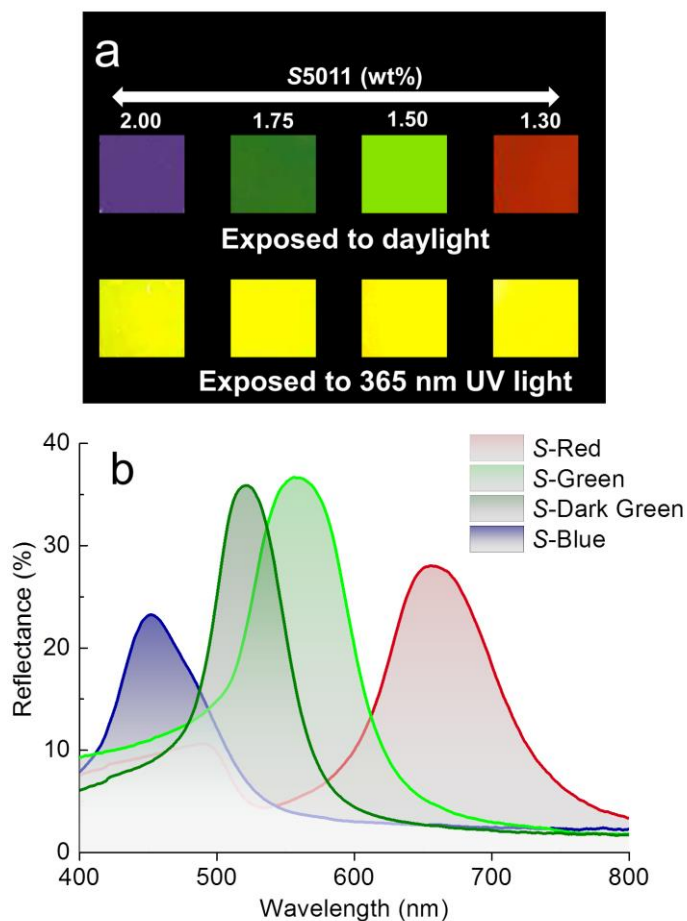


Fig. S7 (a) Photographs and (b) DRUV-vis spectra of *S*-CLC films with different structural colors.

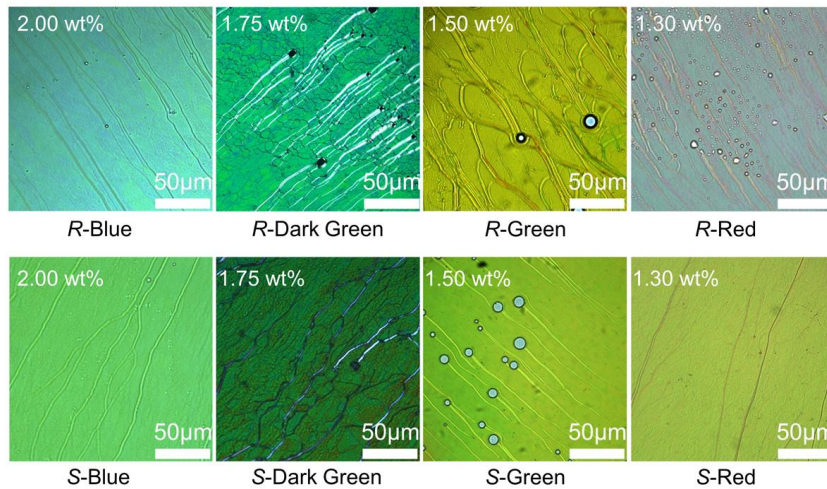


Fig. S8 POM images of C6M with 2 wt% TPE-BF₂acac-MeIP, and 2.00, 1.75, 1.50, and 1.30wt% R/S5011 at 90 °C.

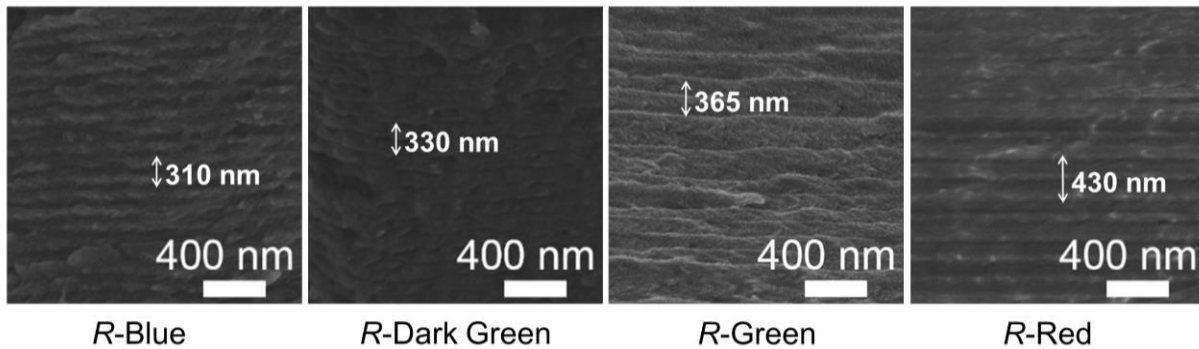


Fig. S9 FESEM images the R-CLC films with 2.00, 1.75, 1.50, and 1.30 wt% R5011.

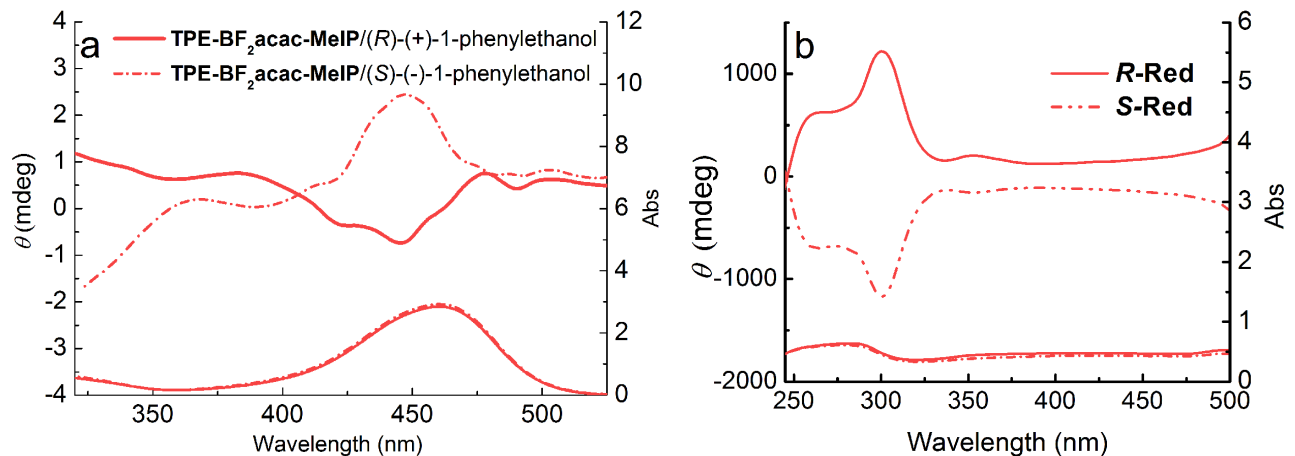


Fig. S10 (a) CD and UV-vis spectra of TPE-BF₂acac-MeIP in (R)-(+)-1-phenylethanol and (S)-(-)-1-phenylethanol (3×10^{-4} M). (b) DRCD and UV-vis spectra of the R/S-Red PSCLC films in the range of 245 ~ 500 nm.

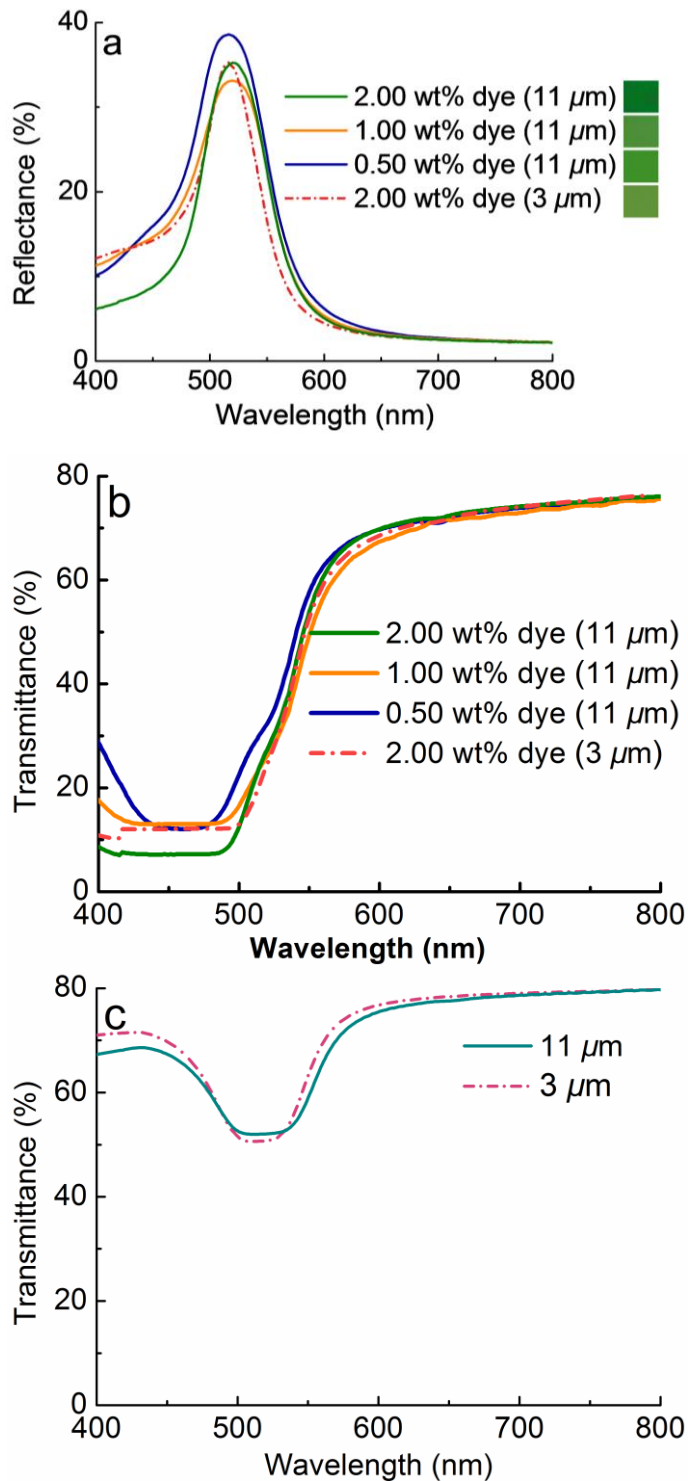


Fig. S11 (a) DRUV-vis spectra and (b) transmittance spectra of with different dye concentrations and thicknesses of *R*-Dark Green PSCLC films. (c) Transmittance spectra of *R*-Dark Green PSCLC films (3 and 11 μm-thickness) without dye.

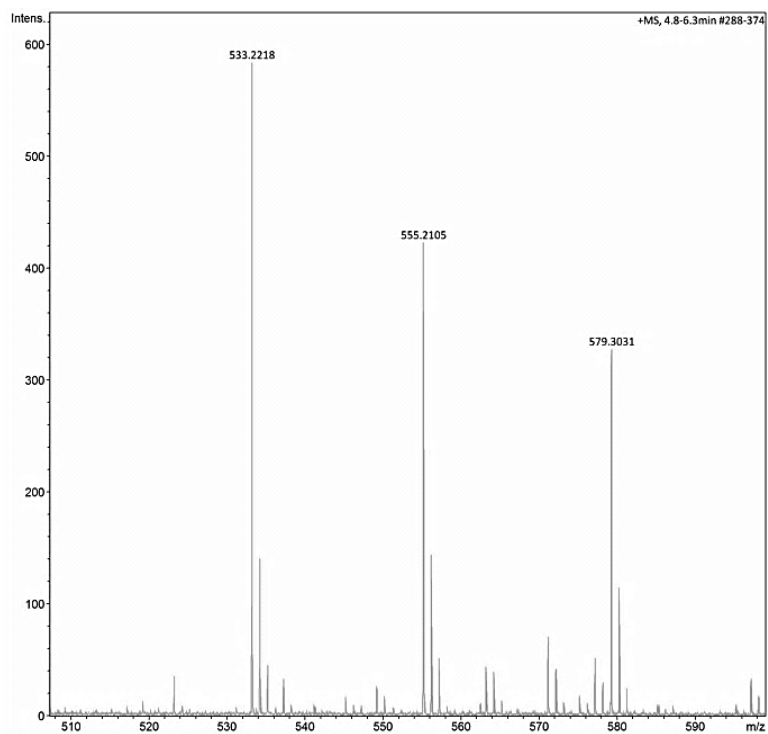


Fig. S12 ESI-MS of TPE-acac-MeIP.

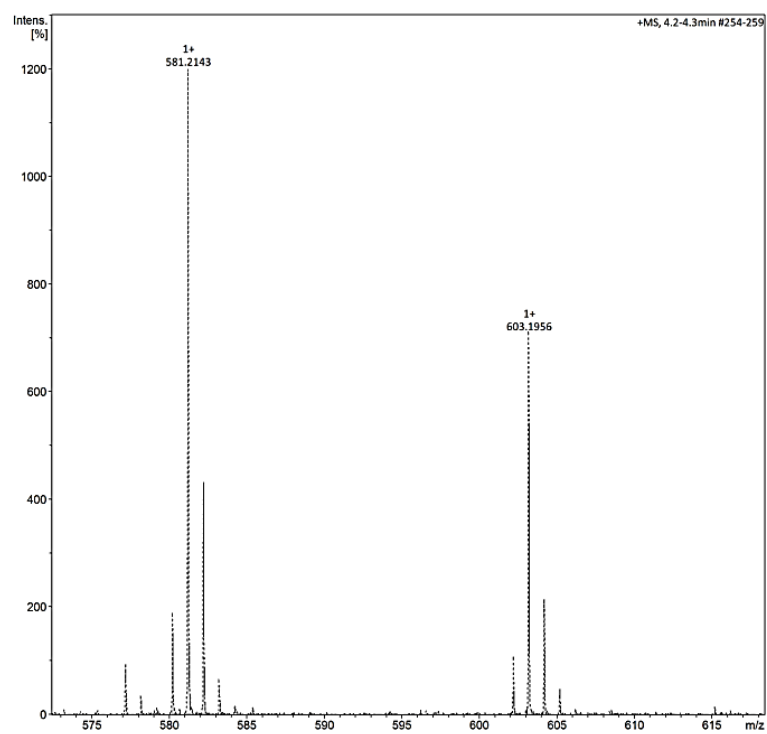


Fig. S13 ESI-MS of TPE-BF₂acac-MeIP.

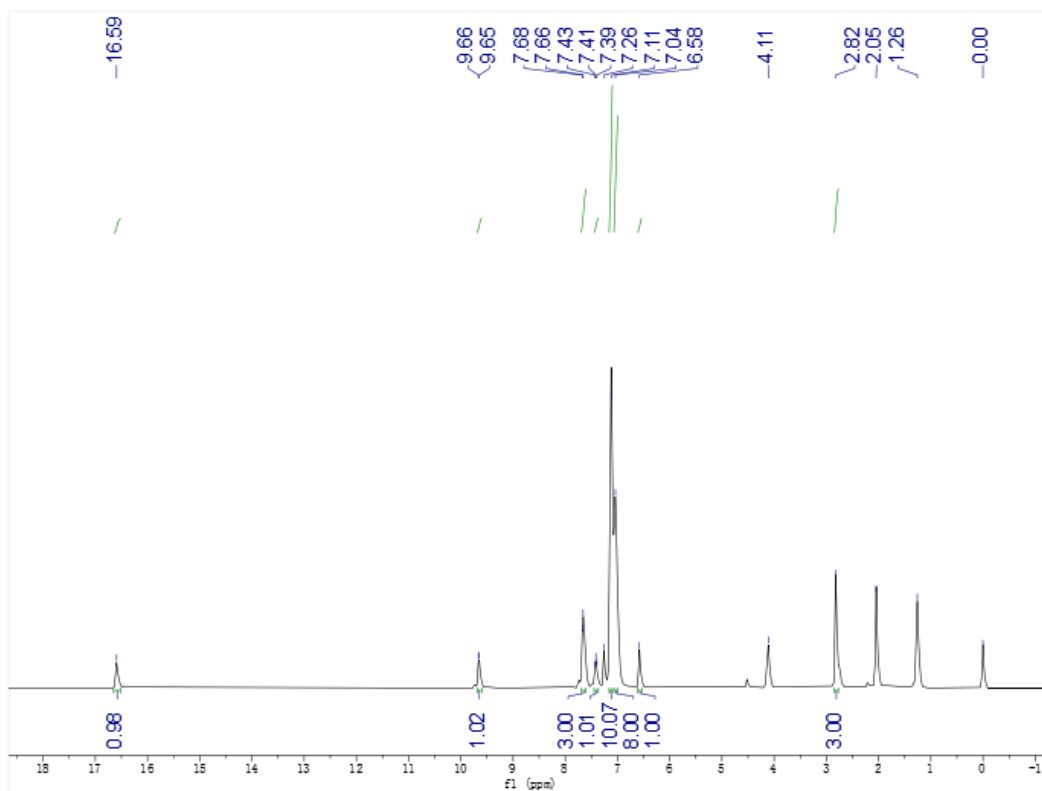


Fig. S14 ^1H NMR (400 MHz, CDCl_3) spectrum of **TPE-acac-MeIP** [δ : 4.11 (CH_2CH_3 in EtOAc), 2.05 (CH_3CO in EtOAc), 1.26 (CH_2CH_3 in EtOAc)].

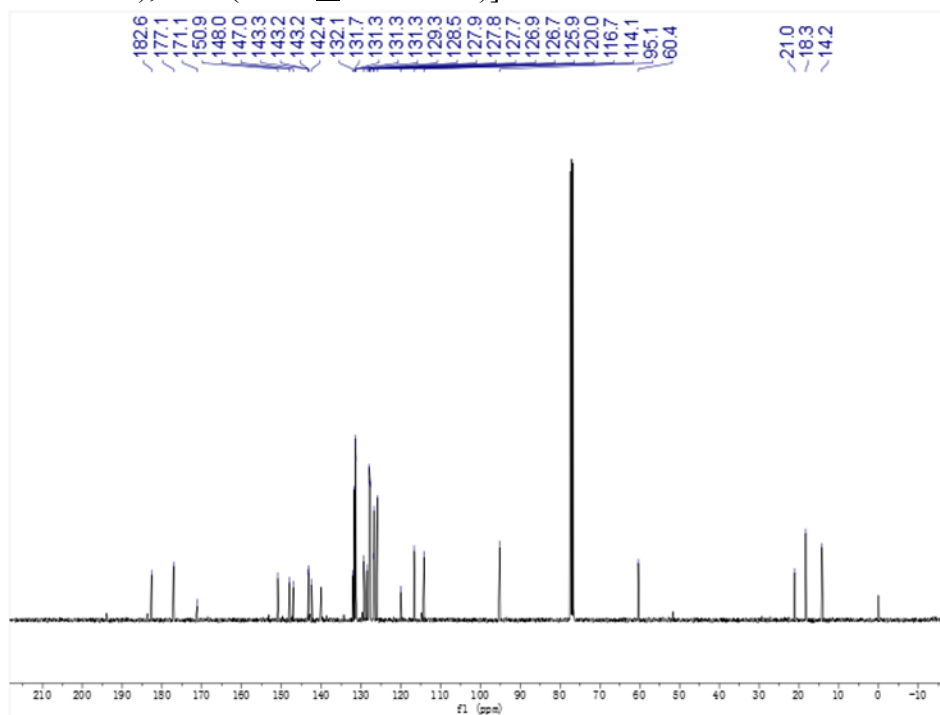


Fig. S15 ^{13}C NMR (100 MHz, CDCl_3) spectrum of **TPE-acac-MeIP** [δ : 171.1 (CO in EtOAc), 60.4 (CH_2 in EtOAc), 21.0 (CH_3CO in EtOAc), 14.2 (CH_3 in EtOAc)].

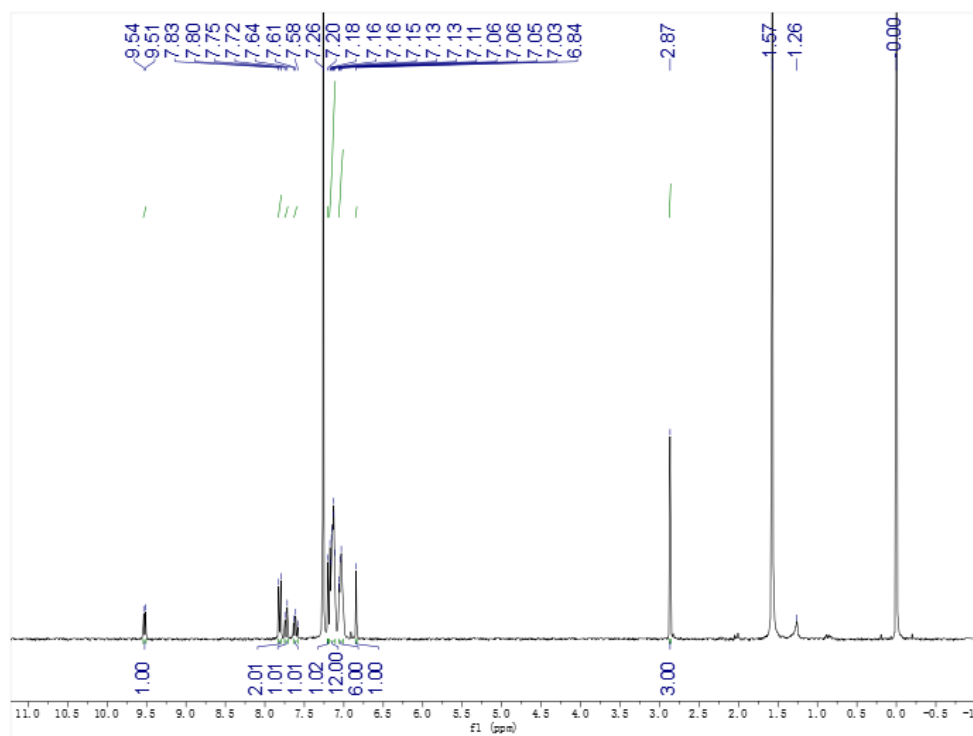


Fig. S16 ^1H NMR (400 MHz, CDCl_3) spectrum of **TPE-BF₂acac-MeIP** [δ : 1.26 (CH_2CH_3 in EtOAc), 1.57 (H_2O)].

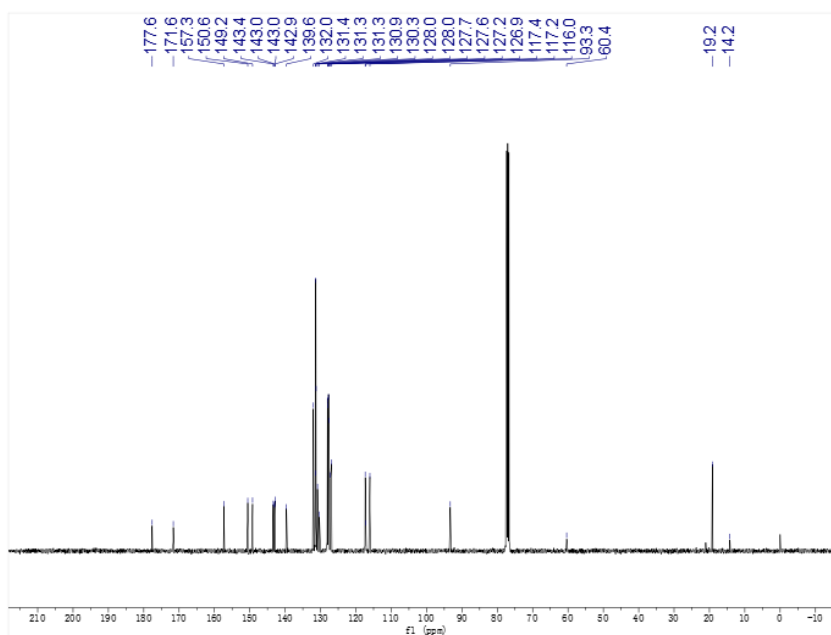


Fig. S17 ^{13}C NMR (101 MHz, CDCl_3) spectrum of **TPE-BF₂acac-MeIP** [δ : 171.1 (C=O in EtOAc), 60.4 (CH_2 in EtOAc), 21.0 (CH_3CO in EtOAc), 14.2 (CH_3 in EtOAc)].

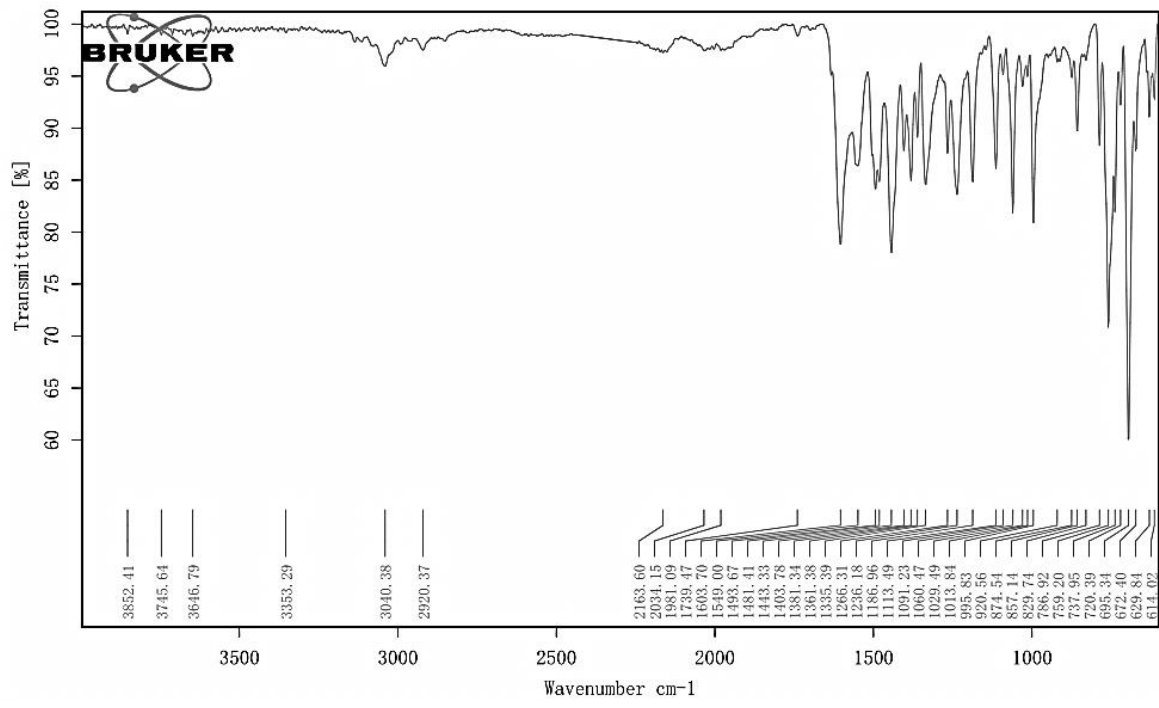


Fig. S18 FT-IR of compound TPE-acac-MeIP.

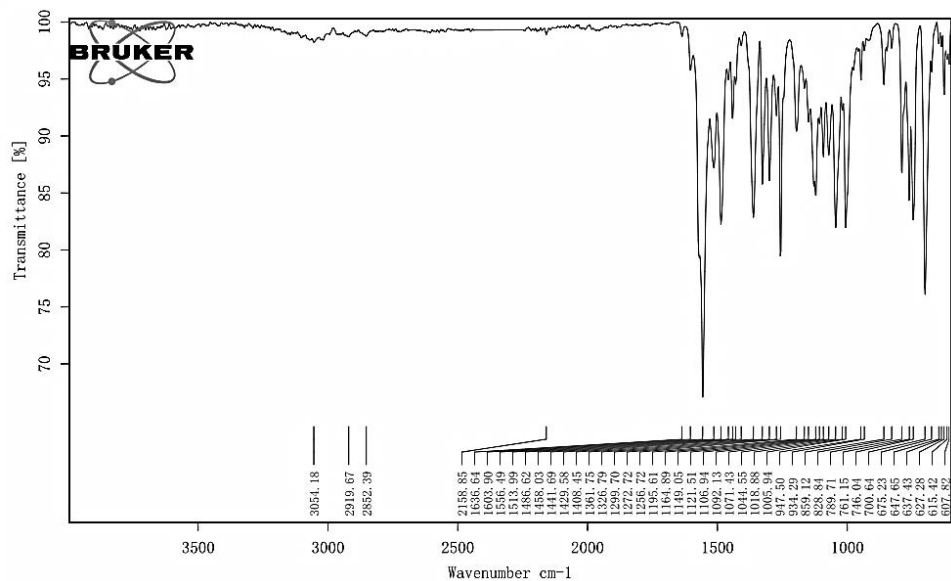


Fig. S19 FT-IR of compound TPE-BF₂acac-MeIP.